THE JOURNAL OF PHYSICAL CHEMISTRY LETTERS
A JOURNAL OF THE AMERICAN CHEMICAL SOCIETY

pubs.acs.org/JPCL Letter

Predicting the Solubility of Organic Energy Storage Materials Based on Functional Group Identity and Substitution Pattern

Madison R. Tuttle,[†] Emma M. Brackman,[†] Farshud Sorourifar, Joel Paulson,* and Shiyu Zhang*

Cite This: *J. Phys. Chem. Lett.* 2023, 14, 1318−1325 Read Online

ACCESS | Metrics & More | Article Recommendations | Supporting Information

ABSTRACT: Organic electrode materials (OEMs) provide sustainable alternatives to conventional electrode materials based on transition metals. However, the application of OEMs in lithium-ion and redox flow batteries requires either low or high solubility. Currently, the identification of new OEM candidates relies on chemical intuition and trial-and-error experimental testing, which is costly and time intensive. Herein, we develop a simple empirical model that predicts the solubility of anthraquinones based on functional group identity and substitution pattern. Within this statistical scaffold, a training set of 18 anthraquinone derivatives allows us to predict the solubility of 808 quinones. Internal and external validations show that our model can predict the solubility of anthraquinones in battery electrolytes within log $S \pm 0.7$, which is a much higher accuracy than existing solubility models. As a demonstration of the utility of our approach, we identified several new anthraquinones with low solubilities and successfully demonstrated their utility experimentally in Li-organic cells.

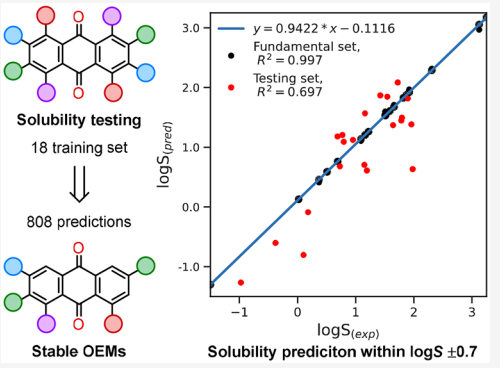

Because fossil fuels represent the largest source of CO_2 emissions, harnessing clean, renewable resources for energy generation has become a global priority in the effort to reach net-zero carbon emissions. Due to the intermittent nature of renewable resources, such as wind, sunlight, and water, a key challenge in the transition to a clean energy economy is the development of grid-scale energy storage systems, such as Li-ion batteries (LIBs)[1] or redox flow batteries (RFBs).[2−4] Organic electrode materials (OEMs) are promising energy storage media in both LIB and RFB systems due to their high structural diversity and synthetic tunability.[5−7] In practice, however, the vast number of OEM variants makes it challenging to identify suitable OEMs with optimal stability, solubility, and redox potentials. Modifications of functional group identity and substitution patterns can result in drastic changes in electronic structures, intra- and intermolecular interactions, and solid-state structure, which influence the performance of OEMs in nonintuitive ways.

Currently, the identification of new OEMs requires trial-and-error synthesis and electrochemical testing (Figure 1A), which are inherently costly and time intensive. To address this issue, quantum chemical calculation, cheminformatic, and machine learning approaches[8,9] have been developed to predict physicochemical properties of OEM candidates, such as redox potentials,[10−13] solubility,[10,13−15] and stability (Figure 1B).[16−19] While the redox potentials of OEMs can be calculated with high precision (often within 50 mV of the experimental values), it is still difficult to forecast the solubility and stability of OEM candidates with reasonable accuracy (Figure 1B). It is a long-standing challenge to predict the solubility of organic molecules. Yet, solubility in the electrolyte is one of the most critical parameters to consider when designing OEMs for LIB and RFB applications—LIBs require OEMs with low solubility to prevent redox shuttling, while RFBs require OEMs with high solubilities to maximize energy density.

Solubility of an organic solid (S_0) is a function of the Gibbs free energy of dissolution (ΔG_{dis}), which is the sum of sublimation energy (ΔG_{sub}) and solvation energy for interactions between solvent and solute (ΔG_{sol}).[20] V_m is the molar volume of the crystal (see Supporting Information).

$$\Delta G_{dis} = \Delta G_{sub} + \Delta G_{sol} = 2.303RT \log(S_0 V_m) \quad (1)$$

Due to a lack of reported crystal structures, estimation of ΔG_{sub} from first-principles is prohibitively costly; therefore, ΔG_{sol} is often used as a proxy for intrinsic solubility due to the ease of calculating solvation energy with quantum chemical methods.[15] However, this approximation leads to poor accuracy, as shown by the work of Cappillino and Mayes et al.[21] To avoid the first principle calculation of ΔG_{dis} altogether, classical cheminformatics methods for predicting the solubility of pharmaceuticals in aqueous environments have also been

Received: January 19, 2023
Accepted: January 26, 2023
Published: February 1, 2023

https://doi.org/10.1021/acs.jpclett.3c00182
J. Phys. Chem. Lett. 2023, 14, 1318−1325

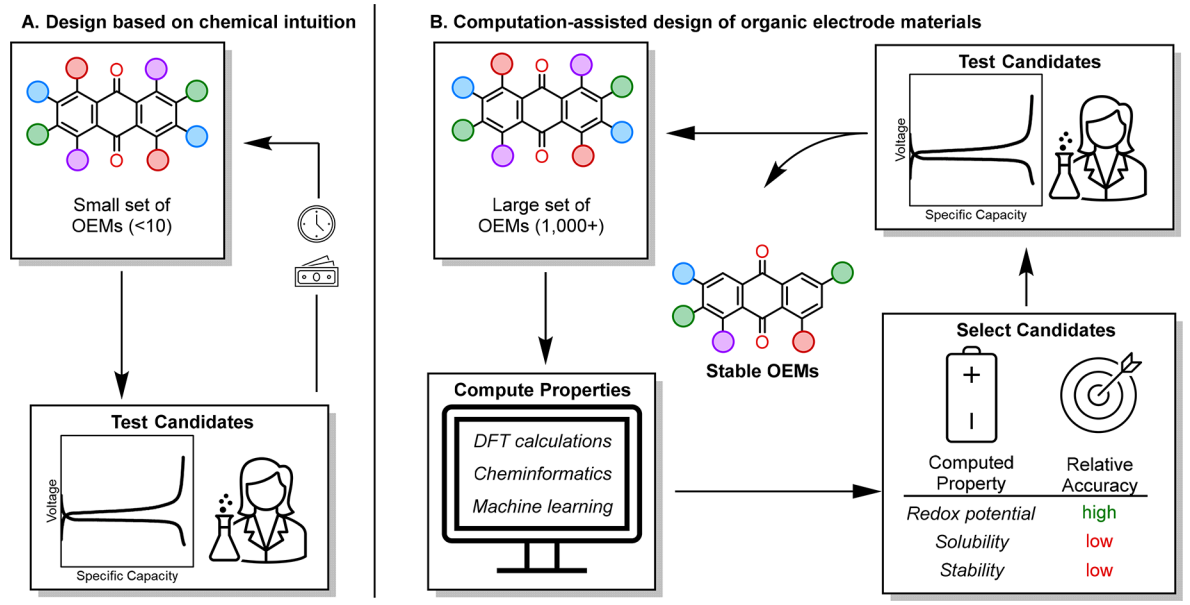

Figure 1. (A) Traditional trial-and-error approach for identifying new OEMs. Small batches of OEM candidates are tested in an iterative process, which is costly and time intensive. (B) Computation-assisted approaches for identifying new OEMs. Relevant properties are computed for vast numbers of OEMs, and candidates with desirable properties are selected for testing. These approaches can predict the redox potential of OEMs with good accuracy but often fail to predict solubility and cycling stability with reasonable accuracy.

applied to select OEM candidates.[10,22] Recently, machine learning has been applied to predict the solubility of solids in aqueous[23−25] and nonaqueous environments.[26,27] However, the accuracy of these models in battery electrolytes has not been verified with experimental solubility data. Sigman and Sanford et al. reported a rare example of an experimentally validated statistical model that predicts the solubility of cyclopropenium dications with high accuracy.[14] However, the parametrization of OEM structures requires sampling and optimization of multiple conformers, making it difficult to forecast new OEMs at a fast pace.

Herein, we develop a statistical model that predicts the solubility of OEMs under battery cycling conditions by considering the influence of functional group identity and substitution pattern on Gibbs free energy of dissolution (ΔG_{dis}). We demonstrate its application with anthraquinone derivatives, a class of redox-active molecules with large structural diversity (>13 000 with reported syntheses). Within this statistical model, the experimental solubilities of 18 quinones allow us to predict that of more than 800 quinones with high confidence without extensive computational calculations. As a demonstration of the utility of this model, we identified several new anthraquinone derivatives with low solubility and successfully demonstrated their utility in Li-organic cells.

Anthraquinone was chosen as the model compound for this study due to its reversible redox behavior and extensive structural diversity. During battery cycling, neutral anthraquinone undergoes a reversible two-electron redox to anthraquinone radical anion and anthraquinone dianion, providing a high theoretical energy storage capacity (Scheme 1). Additionally, the structure of anthraquinone is highly tunable, with up to eight positions that can be synthetically modified and over 13,000 possible substitution patterns and functional group combinations with reported syntheses. This structural tunability ultimately leads to anthraquinone derivatives with a wide range of reported solubilities from ca. 0.61 mM to ca. 1

Scheme 1. Reversible Redox of Anthraquinone

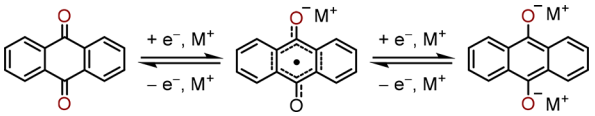

M in dimethoxyethane (DME),[28,29] suggesting that statistical modeling would be instrumental in accelerating the discovery of promising anthraquinone-based OEM candidates for both LIBs and RFB applications.

First, we set out to experimentally measure the solubility of anthraquinone derivatives with a range of functional groups and substitution patterns. To maintain stable cycling in solid-state, the anthraquinone-based OEM candidates must remain insoluble at all redox states. Since the anthraquinone dianion salt generally has a lower solubility than its neutral counterpart,[30−32] the solubility of the neutral anthraquinone species is considered the limiting factor for the application of anthraquinone in solid-state LIBs in this case.[30,33] The experimental solubilities of a set of 38 anthraquinones (Figure 2) with various substitution patterns and functional groups were measured in a common ether-based battery electrolyte (1 M LiTFSI, 0.2 M $LiNO_3$ in 1:1 DME:DOL) using UV−vis spectroscopy (see Supporting Information).

With the solubility of a wide range of anthraquinones under battery cycling conditions in hand, we examined the performance of previous solubility models derived from the Born−Haber cycle of a dissolution process (eq 1).[34] The relationship between the intrinsic solubility (S_0) of an organic solid and the Gibbs free energy of dissolution (ΔG_{dis}) is defined in eq 1. This correlation has been widely applied in understanding the solubility of drug molecules[35−38] and energy storage materials, such as metal complexes,[21] LiO_2, and Li_2O_2.[39] However, while eq 1 is chemically accurate, its practical application is difficult, as the ΔG_{sub} term is computationally expensive and challenging to calculate without a crystal structure.[40] Consequently, many

https://doi.org/10.1021/acs.jpclett.3c00182
J. Phys. Chem. Lett. 2023, 14, 1318−1325

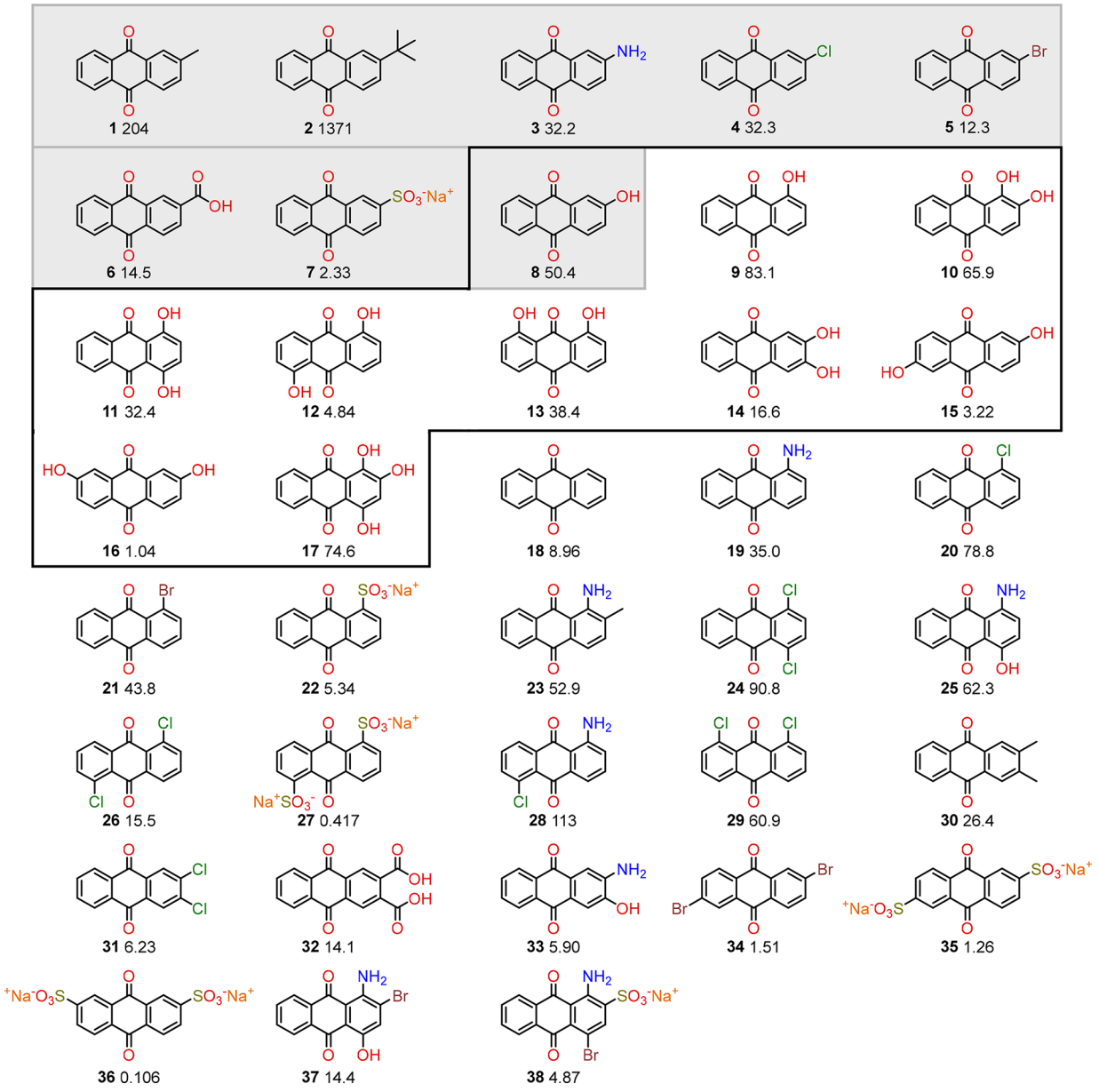

Figure 2. Experimentally determined solubilities (mM) of 38 anthraquinone derivatives in battery electrolyte (1 M LiTFSI, 0.2 M $LiNO_3$ in 1:1 DME:DOL), including the 2-substituted anthraquinones (highlighted in gray) and hydroxy-substituted anthraquinones (outlined in black) used to define substitution identity factor (SIF) and substitution position factor (SPF).

quantitative structure−activity relationships (QSAR) and statistical models ignore ΔG_{sub} and rely on computationally calculated ΔG_{sol} values to estimate solubility.[15,34,41]

Alternatively, some cheminformatics approaches have been developed to predict solubility with experimentally measurable properties. One of the most widely used empirical solubility models in the pharmaceutical industry is the general solubility equation (GSE, eq 2):

$$\log S_{GSE} = 0.5 - 0.01(T_m - 25) - \log P \quad (2)$$

where S_{GSE} is the solubility based on the GSE, T_m is the melting point of the compound, and P is the partition coefficient between an organic solvent and water (see Supporting Information).[34] Another classical empirical solubility model is the Hansen solubility parameters, which estimate the solubility of organic polymers based on their "likeness" to the solvent of choice (R_a), a qualitative expression of the "like-dissolves-like" principle.[42]

Considering the prevalence of these approaches in the literature, we examined the correlation of ΔG_{sol}, S_{GSE}, T_m, log P, and R_a with our experimental solubility data log S in the battery electrolyte. The ΔG_{sol}, ΔG_{hydr}, and log P values were computationally determined for all anthraquinones at a B3LYP/6-31G(d) level of theory with a GD3 empirical dispersion model and an SMD solvent model with either water or 1:1 DME:DOL as the solvents where applicable (Table S2).[41] The T_m values were obtained from literature; log S_{GSE} values were calculated using eq 2. R_a values were calculated using established group contribution methods (see Supporting Information, Tables S2 and S3).[43]

Subsequently, the experimental anthraquinone solubilities were plotted as a function of ΔG_{sol}, log S_{GSE}, log P, T_m, and R_a. As shown in Figure 3A−E, these commonly utilized solubility

https://doi.org/10.1021/acs.jpclett.3c00182
J. Phys. Chem. Lett. 2023, 14, 1318−1325

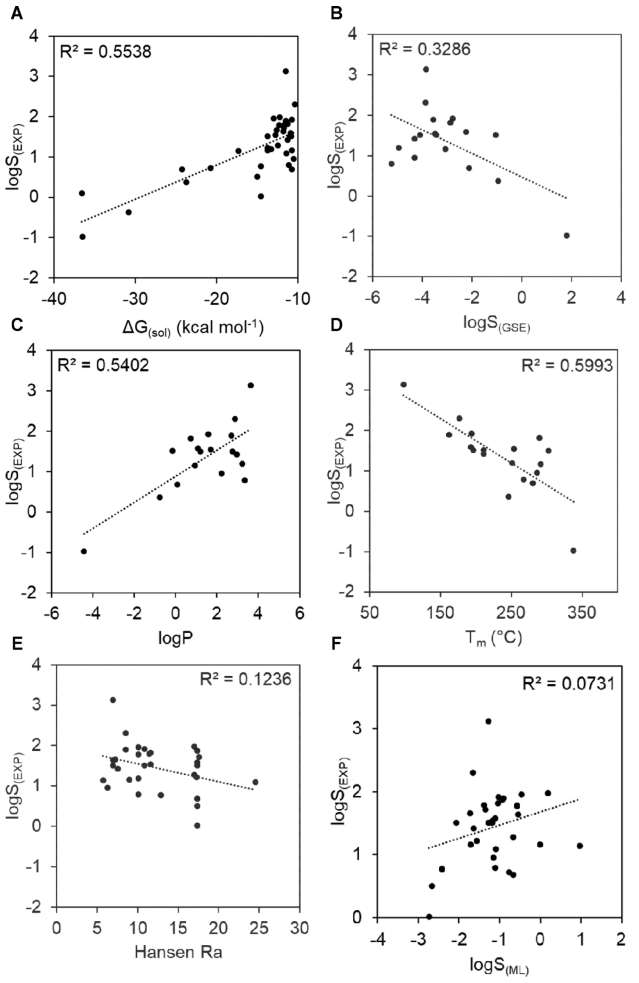

Figure 3. Plots of common solubility descriptors as a function of experimental anthraquinone solubility in 1 M LiTFSI: 0.2 M $LiNO_3$ in 1:1 DME: DOL (Tables S2 and S3). (A) DFT-computed solvation energy ΔG_{sol}, (B) general solubility equation, (C) DFT-computed log *P*, (D) experimental melting point T_m, (E) Hansen solubility parameter R_a, and (F) solubility predicted by ML-model developed by Green et al., log S_{ML}.

descriptors correlate poorly with our experimental anthraquinone solubilities (R^2 = 0.12−0.60), suggesting that they do not predict the solubility of these compounds in battery electrolytes very well. Additionally, we evaluated the machine learning solubility model recently reported by Green,[26] which utilizes simplified molecular-input line-entry system (SMILES) chemical notation inputs to predict the solubility of organic solids. Unfortunately, the parity plot of the model's predictions at 298 K in a 1:1 mixture of DOL and DME against our experimental solubility values shows a low R^2 value of 0.07 (Figure 3F). This method has been shown to be highly successful at predicting the solubility of solids in pure organic solvents; in our case, its poor accuracy is perhaps due to the complex nature of battery electrolyte, which includes lithium salts (e.g., LiTFSI and $LiNO_3$).

As current solubility descriptors, such as ΔG_{sol}, log S_{GSE}, log *P*, T_m, and R_a, and a universal machine learning model failed to capture the experimental solubility of anthraquinones, we considered developing a new method to parametrize the influence of functional groups and substitution pattern on the Gibbs free energy of dissolution (ΔG_{dis}). As shown in Figure 2, the solubility of 2-substituted anthraquinones varies by a factor of 578 from 2.3 mM (*R* = SO_3Na) to 1330 mM (*R* = ^{t}Bu, Figure 2, highlighted in gray). Generally, lower solubility values are observed with more polar and ionic functional groups, consistent with previous studies that show OEMs with strong intermolecular interactions are generally more stable in LIBs.[44,45] However, it is difficult to rationalize the influence of substitution patterns. For example, the solubility of dihydroxyl quinones varies by as much as 20-fold from 3.2 mM (2,6-dihydroxyanthraquinone, **15**) to 65.9 mM (1,2-dihydroxyanthraquinone, **10**), an observation that cannot be easily explained with chemical principles (Figure 2, outlined in black).

Since no intuitive global trend was observed, we considered developing a multivariate linear regression model by parametrizing functional group identity and substitution pattern based on eq 1. Given the small number of data points, we choose to fit the data with a simple straightforward linear model. Our approach was inspired by classical Hammett analysis, which describes reaction rates of a series of related reactions differing only by the substituent of the reactants. In a typical Hammett analysis, only two factors are considered—the substitution position of the functional group (*meta* or *para*) and a constant based on functional group identity (σ value). Although σ values do not carry concrete physical meaning, the Hammett analysis is successful in capturing the trends of a series of chemical reactions that differ only by the identity and pattern of substituents.

Analogously, functional group identity and substitution patterns are expected to influence ΔG_{dis} to different degrees. Therefore, we describe their corresponding contribution to free energy of dissolution solubility (ΔG_{dis}) with eq 3 below:

$$\Delta G_{dis} = \alpha \mathrm{SPF} + \beta \mathrm{SIF} + \gamma \tag{3}$$

where SPF is the substituent position factor, SIF is the substituent identity factor, α, β, and γ are numerical constants that must be calibrated with experimental data such that ΔG_{dis} is the linear combination of SPF and SIF. Since the solubility of organic molecules (S_{FG}, solubility with a certain FG = functional group) is related to ΔG_{dis} as below:

$$\Delta G_{dis} = \log(S_{FG} V_m)$$

Therefore,

$$\log(S_{FG}) = \alpha \mathrm{SPF} + \beta \mathrm{SIF} + \log(V_m^{-1}) + \gamma \tag{4}$$

Next, SPF and SIF are defined using a Hammett-type approach by referencing the experimental solubility of functionalized anthraquinones to that of unsubstituted anthraquinone **18**. Due to the commercial availability of hydroxy-substituted anthraquinones, we chose to define SPF using a set of ten hydroxy-substituted anthraquinones with various substitution patterns (Figure 2, outlined in black). Similar to the Hammett equation, SPF is expressed as the logarithm of the solubility of a substituted anthraquinone with a particular substitution pattern relative to the solubility of unsubstituted anthraquinone:

$$\mathrm{SPF} = \log \frac{S_{SP}}{S_H} \tag{5}$$

where S_{SP} is the solubility (mM) of the hydroxy-substituted anthraquinone with a specified substitution pattern (SP) and S_H is the solubility (mM) of the unsubstituted anthraquinone.

https://doi.org/10.1021/acs.jpclett.3c00182
J. Phys. Chem. Lett. 2023, 14, 1318−1325

For example, the SPF of 1-amino-2-methylanthraquinone **23** can be calculated by the solubility of 1,2-dihydroxyanthraquinone **10** (65.9 mM) and solubility of unsubstituted anthraquinone **18** (8.96 mM). The solubility of 1,2-dihydroxyanthraquinone is used here because it has the same 1,2-substitution pattern as **23** (Figure 4A). The rationale of this approximation is that the molecular shapes of **23** and **10** are similar, which should impact their solubilities to a comparable degree.

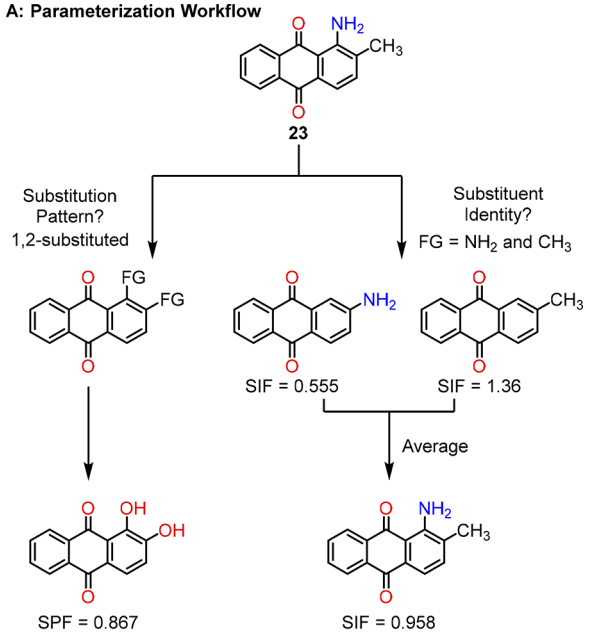

B: Experimental SPF and SIF Values

Substituent Position	$\log\frac{S_{SP}}{S_H}$	Substituent Identity	$\log\frac{S_{SI}}{S_H}$
1-R	0.967	$SO_3^-Na^+$	-0.584
2-R	0.707	NH_2	0.555
1,2-R	0.867	OH	0.707
1,4-R	0.558	CH_3	1.357
1,5-R	-0.263	Cl	0.557
1,8-R	0.632	COOH	0.208
2,3-R	0.267	$C(CH_3)_3$	2.171
2,6-R	-0.445	Br	0.138
2,7-R	-0.933		
1,2,4-R	0.920		

Figure 4. (A) Workflow of parametrization of anthraquinone derivatives based on substituent position factors (SPF) and substituent identity factor (SIF). (B) Summary of experimentally determined SPF and SIF for calculating solubility of anthraquinone derivatives.

Similarly, SIF is defined using a set of eight 2-subsitituted anthraquinones with varying functional groups ($-CH_3$, $-CH(CH_3)_3$, $-NH_2$, $-OH$, $-Cl$, $-Br$, $-COOH$, $-SO_3^-Na^+$). We express SIF as the average of the logarithm of the solubility of a substituted anthraquinone with a particular substituent relative to the solubility of unsubstituted anthraquinone:

$$\mathrm{SIF} = \frac{\log\frac{S_{SI_1}}{S_H} + \ldots + \log\frac{S_{SI_n}}{S_H}}{n} \quad (6)$$

where S_{SI} is the solubility (mM) of the substituted anthraquinone with a specified substituent identity (SI) and n is the number of substituents. Here, the average is taken to describe the average effect of all substituents on intermolecular and solvent interactions. For example, the SIF of 1-amino-2-methylanthraquinone **23** is calculated with the solubility of 2-aminoanthraquinone **3** (S_{NH_2} = 32.2 mM) and the solubility of 2-methylanthraquinone **1** (S_{CH_3} = 204 mM) with n = 2 (Figure 4A). The solubilities of 2-aminoanthraquinone and 2-methylanthraquinone are used to calculate SIF for **23** because they contain the same functional groups. A sample workflow for parametrizing **23** is depicted in Figure 4A. The experimentally determined SPF and SIF values for the fundamental set of anthraquinones are tabulated in Figure 4B.

Using the fundamental set of 18 anthraquinones (**1**−**18**, Figure 2, highlighted in gray and black), we fit the set of parameters $[\alpha, \beta, \gamma]$ to build an initial model. Linear regression was performed on the initial model predictions versus the experimental values, as shown in Figure 2A. The model found is eq 7.

$$\log S = 0.901\cdot\mathrm{SIF} + 0.946\cdot\mathrm{SPF} - 3.38 + \log(1/V_m) \quad (7)$$

The regression yields an R^2 value of 0.997 (Figure 5A). We next used the initial model to predict the solubilities of 20 additional anthraquinones not in the fundamental set (Figure 5A, red points). This external validation shows the model has a R^2 value of 0.816, a slope close to unity (0.98), and an intercept close to 0 (Figure 5A). The robustness of the model was assessed with 3- and 6-fold cross-validation, which affords Q^2 values of 0.639 and 0.563, respectively. These cross-validations consist of dividing the data set into n folds, fitting the model n times on $n - 1$ folds and scoring the model n times on the held-out fold (Figure 5B). The Q^2 values are computed from an n-fold cross-validation using the R^2 scoring metric and reported using an average over the n scores. The high Q^2 values show that the model has a high prediction accuracy on held-out testing points, regardless of which anthraquinones are used for training. Overall, these internal and external validations show that our model can predict solubility with much higher accuracy than general solubility models reported in the literature (Figure 3).

The most practical feature of eq 7 is the separate consideration of substitution pattern and functional group identity. If a small set of solubility values for anthraquinones with various functional groups and various substitution positions can be measured, the solubility of a large set of anthraquinones can be predicted by this simple formula. To demonstrate the effectiveness of this model, we built a data set of 808 anthraquinones for which this model can predict solubility. RDKit was used to find the substitution pattern and substituent identities of each molecule to identify the SPF and SIF. The predicted solubility of 808 anthraquinones is presented in Table S4.

Examination of Table S4 revealed several quinones with very low solubility in our nonaqueous electrolyte, suggesting they could be suitable for LIB application. Theoretically, for OEMs employed in solid-state batteries, low solubility in battery electrolytes should correlate with high cycling stability. Perhaps unsurprisingly, functional groups, such as SO_3Na, COOH, and NH_2, are common in the least soluble anthraquinones predicted by the model due to the effect of intermolecular

https://doi.org/10.1021/acs.jpclett.3c00182
J. Phys. Chem. Lett. 2023, 14, 1318−1325

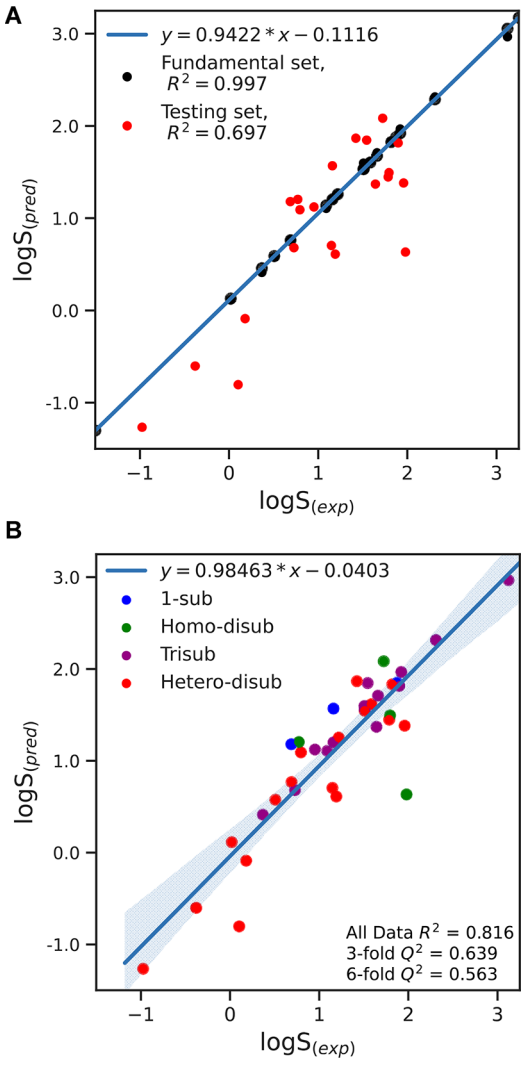

Figure 5. Evaluation of the statistical model for predicting the solubility of anthraquinone. (A) The 18 data points (**1**–**18**) used to define the SIF and SPF are in black. The 20 data points (**19**–**38**) used to validate the model are in red. (B) The data points are color coded based on substitution pattern. The blue region represents 95% confidence interval for the estimated regression line.

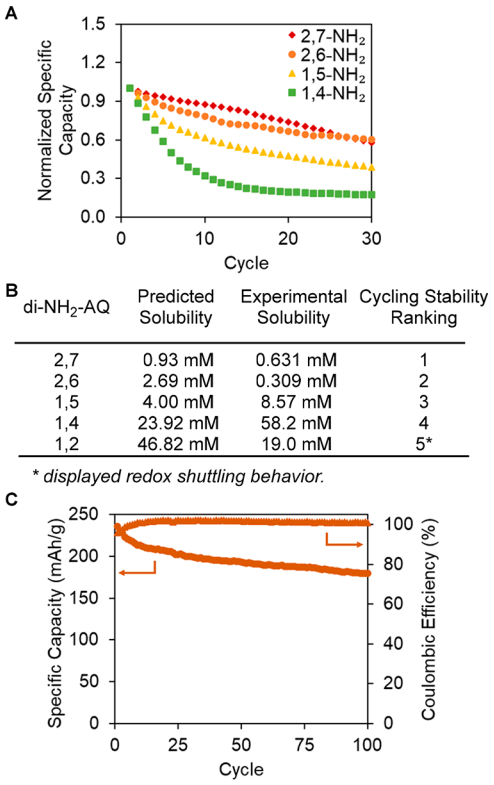

B

di-NH_2-AQ	Predicted Solubility	Experimental Solubility	Cycling Stability Ranking
2,7	0.93 mM	0.631 mM	1
2,6	2.69 mM	0.309 mM	2
1,5	4.00 mM	8.57 mM	3
1,4	23.92 mM	58.2 mM	4
1,2	46.82 mM	19.0 mM	5*

** displayed redox shuttling behavior.*

Figure 6. (A) Comparison of cycling stability for diamino anthraquinone derivatives. (B) Table of predicted solubility and normalized specific capacity values for diamino anthraquinone derivatives after 30 cycles. (C) Galvanostatic cycling data for 1:2 weight ratio of 2,7-NH_2: CMK3 at rate of 0.3C (225.03 mAh g^{-1}).

interactions. However, the model also describes the convoluted influences of substitution patterns and functional groups, which are not obvious based on chemical intuition. Some candidates recommended by our statistical model, such as **17**, **22**, **27**, and **35**, have already shown excellent stability and long cycling lifetimes as OEMs,[46−49] supporting the application of this model for identifying promising OEM candidates.

To further validate our model, we investigated its ability to predict how substitution patterns of OEMs influence solubility, which is a challenging task based on chemical intuition alone. For example, chemical intuition suggests that diaminoanthraquinones should have low solubility due to hydrogen bonding. However, it is unclear which substitution patterns can afford the lowest solubility. Indeed, preliminary coin cell testing of a series of diaminoanthraquinones shows most of them performed poorly in LIBs (Figure 6A). Therefore, chemical intuition alone is not sufficient in identifying the best candidate from a large pool of organic compounds with unknown solubility.

The search process is significantly improved with our model. Our model predicts that the solubility of five diaminoanthraquinones ranks as the following: 2,7- < 2,6- < 1,5- < 1,4- < 1,2-, suggesting that 2,7-diaminoanthraquinone should be prioritized in testing. Indeed, galvanostatic cycling of these diaminoanthraquinone isomers shows that the cycling stability in a Li coin-cell (anode: Li metal, electrolyte: 1 M LiTFSI, 0.2 M $LiNO_3$ in 1:1 DME:DOL) trends with the predicted solubility (Figure 6A, 6B). As the predicted solubilities of the diaminoanthraquinones in battery electrolyte decrease, their stabilities in Li coin cells increase (Figure 6B). Although the stability of organic molecules as cathodes in lithium-ion batteries is influenced by many factors, our work demonstrates that our solubility model can identify promising candidates from a large set of compounds with unknown solubility.

As our model recommends the commercially available 2,7-diaminoanthraquinone as a promising candidate, the cycling conditions in a coin cell were further optimized by tuning the electrode recipe, including conductive carbon and binder. Under optimized conditions (see Supporting Information), galvanostatic cycling was performed at a rate of 0.3C within a voltage window of 1.6−3.0 V. The Li-cell exhibits reversible two-electron cycling with an initial capacity of 235.9 mAh g^{-1}, of which 76.2% was retained after 100 cycles (Figure 6C), representing one of the best-performing anthraquinone cathode materials in LIBs.

In summary, we demonstrated a complete workflow of identifying new organic electrode materials for Li-ion batteries using a simple solubility model. The model can predict the solubility of anthraquinones in a common LIB electrolyte using

https://doi.org/10.1021/acs.jpclett.3c00182
J. Phys. Chem. Lett. 2023, 14, 1318−1325

two easily interpretable structure-based descriptors, substitution position factor (SPF) and substitution identity factor (SIF). The good precision of our model in modeling the solubility of anthraquinones suggests the contribution of the functional group identity and position to ΔG_{sub} and ΔG_{solv} can be considered separately with a QSAR-type of analysis. Importantly, this experimentally calibrated model can be used to predict the solubility of a wide range of anthraquinones with great diversity, including 808 mono-, di-, and trisubstituted anthraquinones that were not measured experimentally. The model and structure-based descriptors defined in this work are straightforward and can be utilized to strategically design anthraquinone structures with both high and low solubilities. Furthermore, this model can potentially be used with other solvents (e.g., aqueous or other nonaqueous solvents) to identify anthraquinone structures suitable for a variety of applications, including both LIBs and RFBs, by measuring α, β, γ, SIF, and SPF in other electrolyte systems. This will be the subject of our future study.

■ ASSOCIATED CONTENT

Supporting Information

The Supporting Information is available free of charge at https://pubs.acs.org/doi/10.1021/acs.jpclett.3c00182.

TExperimental details, including characterization data, spectra, computational procedures, and results (PDF)

■ AUTHOR INFORMATION

Corresponding Authors

Shiyu Zhang − *Department of Chemistry & Biochemistry, The Ohio State University, Columbus, Ohio 43210, United States;* orcid.org/0000-0002-2536-4324; Email: zhang.8941@osu.edu

Joel Paulson − *Department of Chemical and Biomolecular Engineering, The Ohio State University, Columbus, Ohio 43210, United States;* orcid.org/0000-0002-1518-7985; Email: paulson.82@osu.edu

Authors

Madison R. Tuttle − *Department of Chemistry & Biochemistry, The Ohio State University, Columbus, Ohio 43210, United States;* orcid.org/0000-0003-4790-750X

Emma M. Brackman − *Department of Chemistry & Biochemistry, The Ohio State University, Columbus, Ohio 43210, United States*

Farshud Sorourifar − *Department of Chemical and Biomolecular Engineering, The Ohio State University, Columbus, Ohio 43210, United States;* orcid.org/0000-0002-1611-8658

Complete contact information is available at: https://pubs.acs.org/10.1021/acs.jpclett.3c00182

Author Contributions

†These authors contributed equally to this work.

Notes

The authors declare no competing financial interest.

■ ACKNOWLEDGMENTS

This work was supported by the National Science Foundation Graduate Research Fellowship under Grant No. DGE-1343012, the National Science Foundation under CBET-2124604, the Sustainability Institute at Ohio State University, and the Center for Emergent Materials, NSF MRSEC, under award number DMR-2011876.

■ REFERENCES

(1) Poizot, P.; Gaubicher, J.; Renault, S.; Dubois, L.; Liang, Y.; Yao, Y. Opportunities and Challenges for Organic Electrodes in Electrochemical Energy Storage. *Chem. Rev.* **2020**, *120* (14), 6490−6557.

(2) Yang, Z.; Zhang, J.; Kintner-Meyer, M. C. W.; Lu, X.; Choi, D.; Lemmon, J. P.; Liu, J. Electrochemical Energy Storage for Green Grid. *Chem. Rev.* **2011**, *111* (5), 3577−3613.

(3) Feng, R.; Zhang, X.; Murugesan, V.; Hollas, A.; Chen, Y.; Shao, Y.; Walter, E.; Wellala, N. P. N.; Yan, L.; Rosso, K. M.; et al. Reversible Ketone Hydrogenation and Dehydrogenation for Aqueous Organic Redox Flow Batteries. *Science* **2021**, *372* (6544), 836−840.

(4) Lin, K.; Chen, Q.; Gerhardt, M. R.; Tong, L.; Kim, S. B.; Eisenach, L.; Valle, A. W.; Hardee, D.; Gordon, R. G.; Aziz, M. J.; et al. Alkaline Quinone Flow Battery. *Science* **2015**, *349* (6255), 1529−1532.

(5) Liang, Y.; Yao, Y. Positioning Organic Electrode Materials in the Battery Landscape. *Joule* **2018**, *2* (9), 1690−1706.

(6) Luo, J.; Hu, B.; Hu, M.; Zhao, Y.; Liu, T. L. Status and Prospects of Organic Redox Flow Batteries toward Sustainable Energy Storage. *ACS Energy Lett.* **2019**, *4* (9), 2220−2240.

(7) Schon, T. B.; McAllister, B. T.; Li, P.-F.; Seferos, D. S. The Rise of Organic Electrode Materials for Energy Storage. *Chem. Soc. Rev.* **2016**, *45* (22), 6345−6404.

(8) Cheng, L.; Assary, R. S.; Qu, X.; Jain, A.; Ong, S. P.; Rajput, N. N.; Persson, K.; Curtiss, L. A. Accelerating Electrolyte Discovery for Energy Storage with High-Throughput Screening. *J. Phys. Chem. Lett.* **2015**, *6* (2), 283−291.

(9) Agarwal, G.; Doan, H. A.; Robertson, L. A.; Zhang, L.; Assary, R. S. Discovery of Energy Storage Molecular Materials Using Quantum Chemistry-Guided Multiobjective Bayesian Optimization. *Chem. Mater.* **2021**, *33* (20), 8133−8144.

(10) Pineda Flores, S. D.; Martin-Noble, G. C.; Phillips, R. L.; Schrier, J. Bio-Inspired Electroactive Organic Molecules for Aqueous Redox Flow Batteries. 1. Thiophenoquinones. *J. Phys. Chem. C* **2015**, *119* (38), 21800−21809.

(11) Allam, O.; Cho, B. W.; Kim, K. C.; Jang, S. S. Application of DFT-Based Machine Learning for Developing Molecular Electrode Materials in Li-Ion Batteries. *RSC Adv.* **2018**, *8* (69), 39414−39420.

(12) Xu, S.; Liang, J.; Yu, Y.; Liu, R.; Xu, Y.; Zhu, X.; Zhao, Y. Machine Learning-Assisted Discovery of High-Voltage Organic Materials for Rechargeable Batteries. *J. Phys. Chem. C* **2021**, *125* (39), 21352−21358.

(13) Kristensen, S. B.; van Mourik, T.; Pedersen, T. B.; Sørensen, J. L.; Muff, J. Simulation of Electrochemical Properties of Naturally Occurring Quinones. *Sci. Rep.* **2020**, *10* (1), 13571.

(14) Robinson, S. G.; Yan, Y.; Hendriks, K. H.; Sanford, M. S.; Sigman, M. S. Developing a Predictive Solubility Model for Monomeric and Oligomeric Cyclopropenium-Based Flow Battery Catholytes. *J. Am. Chem. Soc.* **2019**, *141* (26), 10171−10176.

(15) Er, S.; Suh, C.; Marshak, M. P.; Aspuru-Guzik, A. Computational Design of Molecules for an All-Quinone Redox Flow Battery. *Chem. Sci.* **2015**, *6* (2), 885−893.

(16) Sevov, C. S.; Hickey, D. P.; Cook, M. E.; Robinson, S. G.; Barnett, S.; Minteer, S. D.; Sigman, M. S.; Sanford, M. S. Physical Organic Approach to Persistent, Cyclable, Low-Potential Electrolytes for Flow Battery Applications. *J. Am. Chem. Soc.* **2017**, *139* (8), 2924−2927.

(17) Lee, B.; Yoo, J.; Kang, K. Predicting the Chemical Reactivity of Organic Materials Using a Machine-Learning Approach. *Chem. Sci.* **2020**, *11* (30), 7813−7822.

(18) Sowndarya S. V., S.; St. John, P. C.; Paton, R. S. A Quantitative Metric for Organic Radical Stability and Persistence Using Thermodynamic and Kinetic Features. *Chem. Sci.* **2021**, *12* (39), 13158−13166.

(19) Assary, R. S.; Zhang, L.; Huang, J.; Curtiss, L. A. Molecular Level Understanding of the Factors Affecting the Stability of

Dimethoxy Benzene Catholyte Candidates from First-Principles Investigations. *J. Phys. Chem. C* **2016**, *120* (27), 14531−14538.
(20) Kuentz, M.; Bergström, C. A. S. Synergistic Computational Modeling Approaches as Team Players in the Game of Solubility Predictions. *J. Pharm. Sci.* **2021**, *110* (1), 22−34.
(21) Visayas, B. R. B.; Pahari, S. K.; Gokoglan, T. C.; Golen, J. A.; Agar, E.; Cappillino, P. J.; Mayes, M. L. Computational and Experimental Investigation of the Effect of Cation Structure on the Solubility of Anionic Flow Battery Active-Materials. *Chem. Sci.* **2021**, *12* (48), 15892−15907.
(22) Hou, T. J.; Xia, K.; Zhang, W.; Xu, X. J. ADME Evaluation in Drug Discovery. 4. Prediction of Aqueous Solubility Based on Atom Contribution Approach. *J. Chem. Inf. Comput. Sci.* **2004**, *44* (1), 266−275.
(23) Lusci, A.; Pollastri, G.; Baldi, P. Deep Architectures and Deep Learning in Chemoinformatics: The Prediction of Aqueous Solubility for Drug-like Molecules. *J. Chem. Inf. Model.* **2013**, *53* (7), 1563−1575.
(24) Cui, Q.; Lu, S.; Ni, B.; Zeng, X.; Tan, Y.; Chen, Y. D.; Zhao, H. Improved Prediction of Aqueous Solubility of Novel Compounds by Going Deeper with Deep Learning. *Front. Oncol.* **2020**, *10*, 121.
(25) Francoeur, P. G.; Koes, D. R. SolTranNet−A Machine Learning Tool for Fast Aqueous Solubility Prediction. *J. Chem. Inf. Model.* **2021**, *61* (6), 2530−2536.
(26) Vermeire, F. H.; Chung, Y.; Green, W. H. Predicting Solubility Limits of Organic Solutes for a Wide Range of Solvents and Temperatures. *J. Am. Chem. Soc.* **2022**, *144* (24), 10785−10797.
(27) Boobier, S.; Hose, D. R. J.; Blacker, A. J.; Nguyen, B. N. Machine Learning with Physicochemical Relationships: Solubility Prediction in Organic Solvents and Water. *Nat. Commun.* **2020**, *11* (1), 5753.
(28) Geysens, P.; Li, Y.; Vankelecom, I.; Fransaer, J.; Binnemans, K. Highly Soluble 1,4-Diaminoanthraquinone Derivative for Nonaqueous Symmetric Redox Flow Batteries. *ACS Sustain. Chem. Eng.* **2020**, *8* (9), 3832−3843.
(29) Wan, W.; Lee, H.; Yu, X.; Wang, C.; Nam, K. W.; Yang, X. Q.; Zhou, H. Tuning the Electrochemical Performances of Anthraquinone Organic Cathode Materials for Li-Ion Batteries through the Sulfonic Sodium Functional Group. *RSC Adv.* **2014**, *4* (38), 19878−19882.
(30) Lu, Y.; Zhang, Q.; Li, L.; Niu, Z.; Chen, J. Design Strategies toward Enhancing the Performance of Organic Electrode Materials in Metal-Ion Batteries. *Chem.* **2018**, *4* (12), 2786−2813.
(31) Zhao, Q.; Guo, C.; Lu, Y.; Liu, L.; Liang, J.; Chen, J. Rechargeable Lithium Batteries with Electrodes of Small Organic Carbonyl Salts and Advanced Electrolytes. *Ind. Eng. Chem. Res.* **2016**, *55*, 5795−5804.
(32) Häupler, B.; Wild, A.; Schubert, U. S. Carbonyls: Powerful Organic Materials for Secondary Batteries. *Adv. Energy Mater.* **2015**, *5* (11), 1402034.
(33) Qin, K.; Huang, J.; Holguin, K.; Luo, C. Recent Advances in Developing Organic Electrode Materials for Multivalent Rechargeable Batteries. *Energy Environ. Sci.* **2020**, *13* (11), 3950−3992.
(34) Bergström, C. A. S.; Larsson, P. Computational Prediction of Drug Solubility in Water-Based Systems: Qualitative and Quantitative Approaches Used in the Current Drug Discovery and Development Setting. *Int. J. Pharm.* **2018**, *540* (1−2), 185−193.
(35) Docherty, R.; Pencheva, K.; Abramov, Y. A. Low Solubility in Drug Development: De-Convoluting the Relative Importance of Solvation and Crystal Packing. *J. Pharm. Pharmacol.* **2015**, *67* (6), 847−856.
(36) Li, L.; Totton, T.; Frenkel, D. Computational Methodology for Solubility Prediction: Application to the Sparingly Soluble Solutes. *J. Chem. Phys.* **2017**, *146* (21), 214110.
(37) Palmer, D. S.; Llinàs, A.; Morao, I.; Day, G. M.; Goodman, J. M.; Glen, R. C.; Mitchell, J. B. O. Predicting Intrinsic Aqueous Solubility by a Thermodynamic Cycle. *Mol. Pharmaceutics* **2008**, *5* (2), 266−279.
(38) Palmer, D. S.; McDonagh, J. L.; Mitchell, J. B. O.; van Mourik, T.; Fedorov, M. V. First-Principles Calculation of the Intrinsic Aqueous Solubility of Crystalline Druglike Molecules. *J. Chem. Theory Comput.* **2012**, *8* (9), 3322−3337.
(39) Cheng, L.; Redfern, P.; Lau, K. C.; Assary, R. S.; Narayanan, B.; Curtiss, L. A. Computational Studies of Solubilities of LiO2 and Li2O2 in Aprotic Solvents. *J. Electrochem. Soc.* **2017**, *164* (11), E3696.
(40) Chen, L.; Bryantsev, V. S. A Density Functional Theory Based Approach for Predicting Melting Points of Ionic Liquids. *Phys. Chem. Chem. Phys.* **2017**, *19* (5), 4114−4124.
(41) Bachman, J. E.; Curtiss, L. A.; Assary, R. S. Investigation of the Redox Chemistry of Anthraquinone Derivatives Using Density Functional Theory. *J. Phys. Chem. A* **2014**, *118* (38), 8852−8860.
(42) Hansen, C. M.*Hansen Solubility Parameters: A User's Handbook*; CRC Press: Boca Raton, FL, 2007.
(43) Stefanis, E.; Panayiotou, C. Prediction of Hansen Solubility Parameters with a New Group-Contribution Method. *Int. J. Thermophys.* **2008**, *29* (2), 568−585.
(44) Tuttle, M. R.; Zhang, S. Bisthiazolyl Quinones: Stabilizing Organic Electrode Materials with Sulfur-Rich Thiazyl Motifs. *Chem. Mater.* **2020**, *32* (1), 255−261.
(45) Tuttle, M. R.; Davis, S. T.; Zhang, S. Synergistic Effect of Hydrogen Bonding and $\pi-\pi$ Stacking Enables Long Cycle Life in Organic Electrode Materials. *ACS Energy Lett.* **2021**, *6*, 643−649.
(46) Reddy, A. L. M.; Nagarajan, S.; Chumyim, P.; Gowda, S. R.; Pradhan, P.; Jadhav, S. R.; Dubey, M.; John, G.; Ajayan, P. M. Lithium Storage Mechanisms in Purpurin Based Organic Lithium Ion Battery Electrodes. *Sci. Rep.* **2012**, *2* (1), 960.
(47) Liu, W.; Tang, W.; Zhang, X. P.; Hu, Y.; Wang, X.; Yan, Y.; Xu, L.; Fan, C. A Polyanionic Anthraquinone Organic Cathode for Pure Small-Molecule Organic Li-Ion Batteries. *Int. J. Hydrogen Energy* **2021**, *46* (74), 36801−36810.
(48) Tang, W.; Liang, R.; Li, D.; Yu, Q.; Hu, J.; Cao, B.; Fan, C. Highly Stable and High Rate-Performance Na-Ion Batteries Using Polyanionic Anthraquinone as the Organic Cathode. *ChemSusChem* **2019**, *12* (10), 2181−2185.
(49) Wan, W.; Lee, H.; Yu, X.; Wang, C.; Nam, K.-W.; Yang, X.-Q.; Zhou, H. Tuning the Electrochemical Performances of Anthraquinone Organic Cathode Materials for Li-Ion Batteries through the Sulfonic Sodium Functional Group. *RSC Adv.* **2014**, *4* (38), 19878−19882.

https://doi.org/10.1021/acs.jpclett.3c00182
J. Phys. Chem. Lett. 2023, 14, 1318−1325